



# Use of polymeric CXCR4 inhibitors as siRNA delivery vehicles for the treatment of acute myeloid leukemia

Yiqian Wang<sup>1</sup> · Ying Xie<sup>2</sup> · Jacob Williams<sup>1</sup> · Yu Hang<sup>2</sup> · Lisa Richter<sup>1</sup> · Michelle Becker<sup>1</sup> · Catalina Amador<sup>3</sup> · David Oupicky<sup>2</sup> · R. Katherine Hyde<sup>1</sup>

Received: 7 February 2019 / Revised: 11 April 2019 / Accepted: 13 April 2019 / Published online: 26 April 2019  
© Springer Nature America, Inc. 2019

## Abstract

Acute myeloid leukemia (AML) is the most common type of acute leukemia in adults and is associated with poor long-term survival often owing to relapse. Current treatments for AML are associated with considerable toxicity and are frequently not effective after relapse. Thus, it is important to develop novel therapeutic strategies. Short interfering RNA (siRNA)-based therapeutics targeting key oncogenes have been proposed as treatments for AML. We recently developed novel siRNA delivery polycations (PCX) based on AMD3100 (plerixafor), an FDA-approved inhibitor of the CXC chemokine receptor 4 (CXCR4). Inhibitors of CXCR4 have been shown to sensitize leukemia cells to chemotherapy. Therefore, PCX has the potential to target leukemia cells via two mechanisms: inhibition of CXCR4 and delivery of siRNAs against critical genes. In this report, we show that PCX exerts a cytotoxic effect on leukemia cells more effectively than other CXCR4 inhibitors, including AMD3100. In addition, we show that PCX can deliver siRNAs against the transcription factor RUNX1 to mouse and human leukemia cells. Overall, our study provides the first evidence that dual-function PCX/siRNA nanoparticles can simultaneously inhibit CXCR4 and deliver siRNAs, targeting key oncogenes in leukemia cells and that PCX/siRNA has clinical potential for the treatment of AML.

## Introduction

Acute myeloid leukemia (AML) is a heterogeneous clonal disorder characterized by the accumulation of immature myeloid cells in the bone marrow. It is the most common type of acute leukemia in adults, and its incidence increases

with age [1–4]. Current treatments for AML include high-dose chemotherapy and stem cell transplantation, both of which are associated with significant morbidity and mortality [1, 5, 6]. In addition, even with optimal treatment, AML patients frequently relapse, which in part explains why the prognosis for AML remains poor with the overall 5-year survival rate of only 27% [6]. Thus, there is an urgent need to develop novel therapeutics to improve treatment outcomes for patients with AML.

Compared with other cancers, AML has a low mutational burden [7, 8]. For this reason, AML cells are likely dependent on a relatively small number of oncoproteins. However, many AML mutations involve transcription factors, which are difficult to target with traditional small molecules. For example, efforts to develop inhibitors of RUNX1, one of the most commonly mutated genes in AML, have shown potential in tissue culture and mouse models, but there have not yet been any compounds identified suitable for use in humans [9–11]. Small interfering RNAs (siRNAs) have the potential to overcome these limitations as they are based on nucleic acid sequence, and not protein structure. Successfully targeted delivery of siRNAs against specific oncogenes has been reported in a variety of

**Supplementary information** The online version of this article (<https://doi.org/10.1038/s41417-019-0095-9>) contains supplementary material, which is available to authorized users.

✉ R. Katherine Hyde  
kate.hyde@unmc.edu

<sup>1</sup> Department of Biochemistry and Molecular Biology, and Fred & Pamela Buffett Cancer Center, University of Nebraska Medical Center, Omaha, NE, USA

<sup>2</sup> Center for Drug Delivery and Nanomedicine, Department of Pharmaceutical Sciences, University of Nebraska Medical Center, Omaha, NE, USA

<sup>3</sup> Department of Pathology and Microbiology, University of Nebraska Medical Center, Omaha, NE, USA

different types of cancer, including AML [12–15]. However, the clinical translation of such therapies has been difficult, mainly owing to nuclease degradation during siRNA delivery [16, 17]. Thus, strategies for enhancing cellular uptake and allowing siRNA to specifically reach the target cells are required.

We have recently developed polymeric CXCR4 antagonists (PCX), which are capable of inhibiting CXC chemokine receptor 4 (CXCR4) and carrying siRNA simultaneously [18–20]. PCX was synthesized from AMD3100 (plerixafor), an FDA-approved CXCR4 inhibitor, and modified with cholesterol for better systemic delivery (Fig. 1a, b) [19, 20]. CXCR4 is expressed on a variety of AML subtypes, and AMD3100 is currently being tested for its ability to mobilize leukemia stem cells (LSCs) from the bone marrow, as a way of making them more susceptible to traditional chemotherapy [21–24]. Therefore, PCX/siRNA nanoparticles have the potential to target AML cells by two mechanisms: inhibition of CXCR4 and delivery of knockdown constructs against critical oncogenes.

In our study, we show that PCX is suitable for use in combination with traditional chemotherapy, and that PCX has a potent cytotoxic effect on AML cells in vitro, which is not observed with other CXCR4 inhibitors. Furthermore, using siRNA targeting RUNX1, a transcription factor required in a variety of different AML subtypes, we show that PCX/siRUNX1 polyplexes efficiently knock down *RUNX1* expression in both mouse and human leukemia cells. Importantly, PCX/siRUNX1 had a greater effect on cell viability compared with the control. Collectively, our data demonstrate that CXCR4-targeted siRNA nanoparticles have potential as a novel treatment for AML.

## Results

### PCX decreases leukemia cell viability in vitro

To examine the potential of PCX in AML, we used a knock-in mouse model of inversion [16] [*inv(16)*] AML expressing a conditional allele of full-length *Cbfb-MYH11* from the endogenous *Cbfb* locus (*Cbfb*<sup>+/*56M*</sup>) paired with the inducible *Mx1-Cre* transgene [25, 26]. This knock-in mouse model expresses the initiating oncogene, *Cbfb-MYH11*, at physiologically relevant levels and develops a disease that closely resembles human *inv(16)* AML, making it a useful model to test PCX. To verify that CXCR4 is expressed on *Cbfb-MYH11*<sup>+</sup> leukemia cells, we stained cells derived from three independent primary *Cbfb-MYH11*<sup>+/*56M*</sup>, *Mx1-Cre*<sup>+</sup> mice for CXCR4. We also included CSF2RB, a marker we previously showed distinguishes LSCs from non-LSCs in this model [27, 28]. We found that the majority of LSCs and non-LSCs from both bone marrow and spleen express CXCR4 (Fig. 2a). This indicates that CXCR4 is highly expressed in leukemia cells from this mouse model.

In clinical trials, CXCR4 inhibitors have been shown to improve outcomes when given in combination with conventional chemotherapy [22–24]. To ensure that PCX does not diminish the effect of chemotherapy drugs, we treated *Cbfb-MYH11*<sup>+</sup> leukemia cells from three independent *Cbfb-MYH11*<sup>+/*56M*</sup>, *Mx1-Cre*<sup>+</sup> mice with cytarabine (AraC) or doxorubicin (DOX) alone, or in combination with PCX. We used PCX at a dose of 2.1 µg/mL, which we previously showed effectively inhibits CXCR4 [29]. After 48 h, viability was measured by flow cytometry using 4',6-diamidino-2-phenylindole (DAPI). We found that all treatment groups showed decreased viability as compared with untreated cells (Fig. 2b). The combination of PCX with

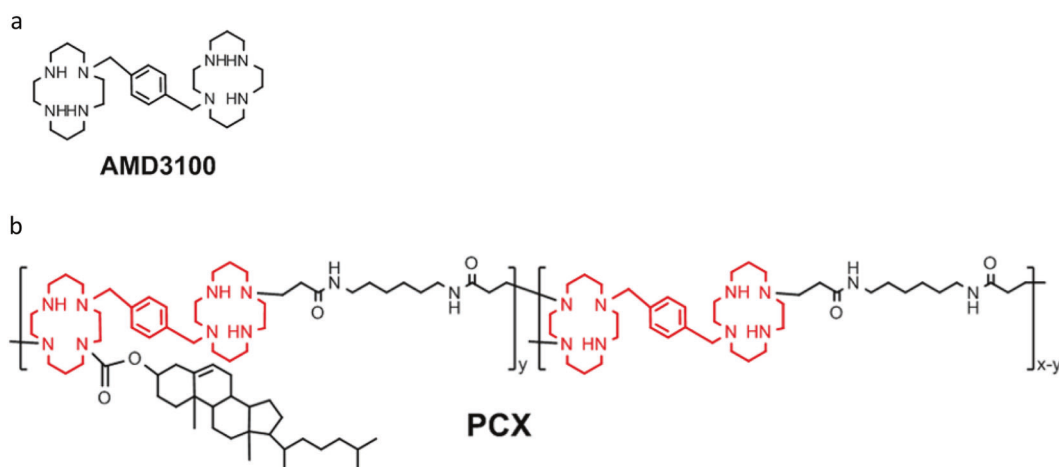


**Fig. 1** Chemical structure of **a** AMD3100 (Plerixafor) and **b** PCX

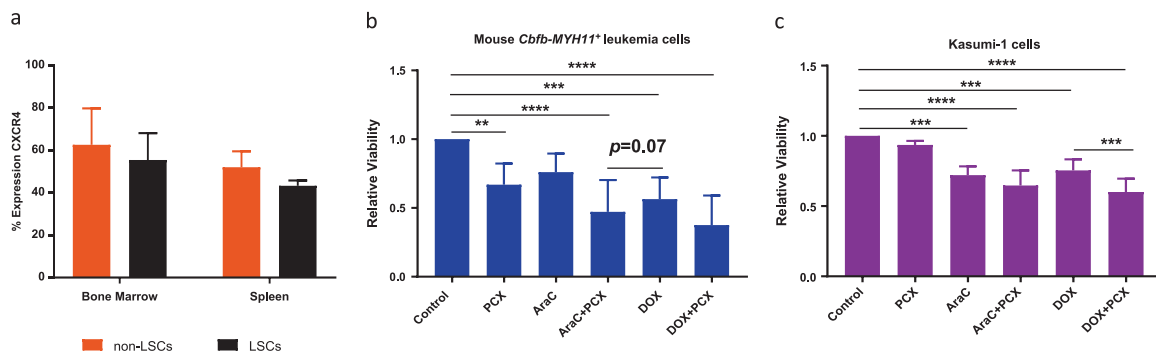


**Fig. 2** CXCR4 is expressed on *Cbfb-MYH11*<sup>+</sup> leukemia cells, and PCX decreased leukemia cell survival in vitro. **a** Bar graph showing the percentage of *Cbfb-MYH11*<sup>+</sup> LSCs and non-LSCs that express the CXCR4 receptor in bone marrow and spleen ( $n = 3$ ). **b**, **c** Bar graphs showing the relative viability of mouse *Cbfb-MYH11*<sup>+</sup> leukemia cells

( $n = 8$ ) and Kasumi-1 cells ( $n = 5$ ) incubated with PCX (2.1  $\mu\text{g}/\text{mL}$ ) alone or combination with 8  $\mu\text{M}$  cytarabine (AraC) or 2  $\mu\text{M}$  doxorubicin (DOX) for 48 h in culture. Data are shown as mean  $\pm$  SD. \*\* $p < 0.01$ ; \*\*\* $p < 0.001$ ; \*\*\*\* $p < 0.0001$

either AraC or DOX showed a trend toward decreased viability as compared with either chemotherapy drug alone, although this difference was not statistically significant. Importantly, PCX did not rescue the decrease in viability caused by either AraC or DOX alone, indicating that PCX does not block the activity of frontline chemotherapeutic agents. To confirm that PCX has similar effects in human leukemia cells, we used the patient-derived cell lines, Kasumi-1, which has the t(8;21) translocation and ME-1 which has inv(16). We found that PCX did not block the decreased viability caused by either AraC or DOX, and that the combination of DOX and PCX caused a statistically significant decrease in viability as compared with DOX alone in Kasumi-1 cells (Fig. 2c). We also saw that PCX caused a trend toward decreased viability without blocking the activity of either AraC or DOX in ME-1 cells (Supplemental Fig. S1). Overall, our data imply that PCX has no adverse effect on the efficiency of chemotherapy and could be used in combination with conventional drugs in AML patients.

### PCX has novel anti-leukemia activities

Our finding that treatment with PCX alone caused decreased leukemia cell viability in vitro is surprising, as the monomeric form of PCX, AMD3100, is not thought to have anti-leukemia activity on its own [21]. This implies that the polymeric form has novel activities. To test the possibility, leukemia cells from three independent *Cbfb-MYH11*<sup>+56M</sup>, *Mxl-Cre*<sup>+</sup> mice were cultured with increasing concentrations of PCX or AMD3100. We also tested two different synthetic peptide CXCR4 inhibitors, BKT140 and LY2510924 [30–35]. After 48 h of treatment, viability was measured by flow cytometry using DAPI. We found that the viability was significantly decreased by PCX in a concentration-dependent fashion. Interestingly, none of the other CXCR4 inhibitors significantly affected cell viability,

even at doses 10–20 times greater than that of PCX (Fig. 3a). To test whether PCX caused decreased viability via apoptosis, we stained cells with Annexin V. We found that treatment with PCX, but not the other CXCR4 inhibitors, increased Annexin V staining in a concentration-dependent fashion (Fig. 3b). To test the effect of PCX on normal cells, we first examined CXCR4 expression on normal cells. We found that CXCR4 is highly expressed on both normal bone marrow and spleen cells (Supplemental Fig. S2a). We next treated bone marrow and spleen cells from wild-type mice with PCX in culture. For comparison, leukemia cells from three independent *Cbfb-MYH11*<sup>+56M</sup>, *Mxl-Cre*<sup>+</sup> mice were incubated with PCX in parallel. After 24 h of treatment, we stained cells with DAPI and Annexin V. At this time point, we found that PCX caused a trend towards decreased viability and a statistically significant increase in Annexin V staining in mouse leukemia cells compared with untreated cells, consistent with our previous observations. Importantly, PCX did not affect viability or Annexin V staining in normal bone marrow or spleen cells as compared with control (Supplementary Fig. S2b, c). These results indicate that PCX does not cause cell death in normal hematopoietic cells. To determine whether PCX cytotoxicity is associated with increased differentiation, we stained cells for Mac-1 and Gr-1, markers of mature myeloid cells. We found that PCX induced a trend toward increased Mac-1 and Gr-1 expression, as compared with the untreated cells (Fig. 3c and Supplementary Fig. S3a, b). We observed no difference in either Mac-1 or Gr-1 expression with the other CXCR4 inhibitors. Cytospins of cells confirmed slight features of differentiation with PCX treated cells showing more abundant cytoplasm with increased granularity (Fig. 3d). Overall, our findings indicate that PCX exhibits a more potent anti-leukemia activity in vitro as compared with other CXCR4 inhibitors, which further supports the use of PCX as an anti-leukemic therapy.

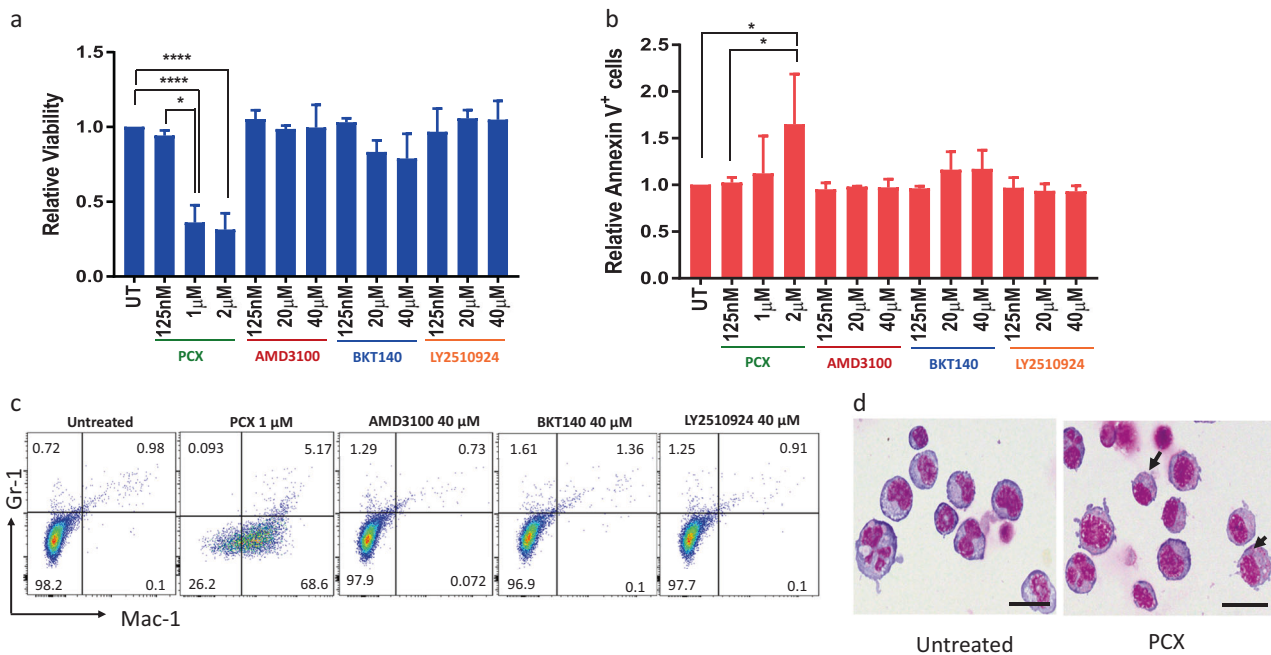


**Fig. 3** PCX has novel anti-leukemia activity. **a** Bar graph showing the relative viability of *Cbfb-MYH11*<sup>+</sup> leukemia cells treated with the indicated drugs for 48 h in culture with different concentrations, as indicated ( $n = 3$ ). **b** Bar graph showing the relative Annexin V staining of *Cbfb-MYH11*<sup>+</sup> leukemia cells treated with the indicated drugs for 48 h in culture ( $n = 3$ ). **c** Representative FACS plots gated on Mac-1 and Gr-1 in *Cbfb-MYH11*<sup>+</sup> leukemia cells treated with the indicated

concentrations of CXCR4 inhibitors for 48 h in culture. **d** Cells treated with vehicle or PCX (1 μM) were adhered to slides using a cytopsin, stained with Wright-Giemsa and imaged at  $\times 100$  magnification. Black arrowhead indicates the presence of cytoplasmic granules. Scale bar: 20 μm. UT, Untreated. Data are shown as mean  $\pm$  SD. \*  $p < 0.05$ ; \*\*\*\*  $p < 0.0001$

### Runx1 knockdown increased apoptosis and decreased colony-forming ability in *Cbfb-MYH11*<sup>+</sup> leukemia cells

In addition to inhibiting CXCR4, PCX also has the ability to encapsulate and deliver siRNAs against critical genes. In previous work, we showed that the transcription factor RUNX1 is required for the development of *Cbfb-MYH11*<sup>+</sup> leukemia, implying that RUNX1 is an appropriate knockdown target in frank leukemia cells [26]. Before testing this possibility, we first confirmed that Runx1 protein and mRNA expression levels on normal tissues and *Cbfb-MYH11*<sup>+</sup> leukemia cells. We found that Runx1 is highly expressed in normal bone marrow and spleen cells, as well as the LSCs and non-LSCs harvested from both the bone marrow and spleen of leukemic *Cbfb-MYH11*<sup>+</sup> mice (Fig. 4a and Supplemental Fig. S4a, b). To test if knockdown of *Runx1* expression affects leukemia cell survival, we transduced leukemia cells from three independent *Cbfb-MYH11*<sup>+/56M</sup>, *Mx1-Cre*<sup>+</sup> mice with lentiviral vectors expressing either an shRNA targeting *Runx1* (shRunx1) or a scrambled shRNA (shSCR), and DsRed. After 48 h of transduction, we sorted cells for DsRed expression. To test the knockdown efficiency of shRunx1, the mRNA and protein expression levels of *Runx1* were examined by quantitative real-time polymerase chain reaction (RT-PCR) and western blot

analysis in sorted leukemia cells. We found that *Runx1* mRNA and protein were significantly lower in cells transduced with shRunx1 as compared with shSCR-transduced cells (Fig. 4b, c). To test the effect of *Runx1* knockdown on apoptosis, we used Annexin V staining. shRunx1-transduced cells showed significantly higher Annexin V staining as compared with cells transduced with shSCR (Fig. 4d). To determine the effect of *Runx1* knockdown on LSC activity, we performed colony formation assays. Equal numbers of *Cbfb-MYH11*<sup>+</sup> leukemia cells transduced with shSCR or shRunx1 were plated in methylcellulose. After 14 days of culture, colonies were counted. We found that leukemia cells transduced with shRunx1 produced significantly fewer colonies compared with the control group (Fig. 4e). These results indicate that the knockdown of *Runx1* increases apoptosis and leads to decreased colony-forming ability of *Cbfb-MYH11*<sup>+</sup> leukemia cells in vitro, and that Runx1 is an appropriate target to test the ability of PCX to deliver knockdown constructs.

### PCX condenses siRNA to form nanoparticles

The capability of PCX to form nanoparticles with siRNA was first validated using a gel retardation assay. Nanoparticles were prepared by mixing PCX with siRNA solution at increasing PCX/siRNA ratios. PCX fully

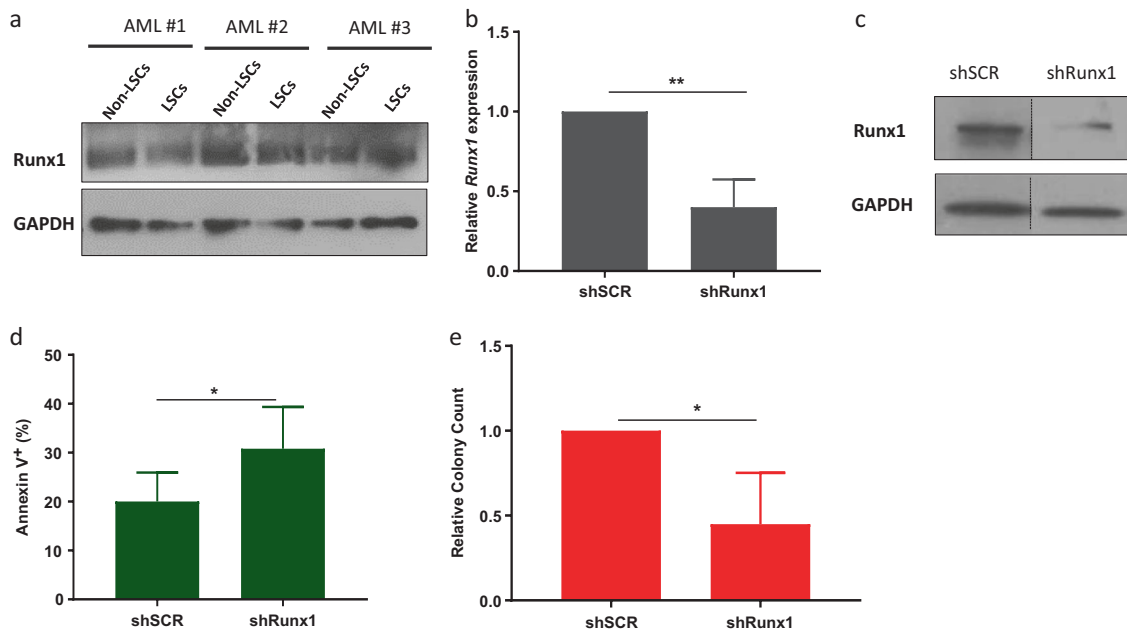


**Fig. 4** *Runx1* is required in transformed *Cbfb-MYH11*<sup>+</sup> leukemia cells. **a** Western blot of *Runx1* and the loading control *GAPDH* in *Cbfb-MYH11*<sup>+</sup> LSCs and non-LSC harvested from the spleen. **b** Bar graph showing the fold change in mRNA expression of *Runx1* in *Cbfb-MYH11*<sup>+</sup> leukemia cells infected with an shRNA targeting *Runx1* (shRunx1) or a scrambled control shRNA (shSCR) ( $n = 4$ ). **c** Western blot of *Runx1* and the loading control *GAPDH* in *Cbfb-MYH11*<sup>+</sup> leukemia cells infected with shRunx1 and shSCR; dotted line indicates

the division between two different parts of the same blot. **d** Bar graph showing the percentage of Annexin V<sup>+</sup> leukemia cells 48 h after transduction with lentiviral vectors expressing the indicated shRNA constructs ( $n = 5$ ). **e** Bar graph showing the relative number of colonies formed from leukemia cells infected with shRunx1 or shSCR after 14 days in culture ( $n = 3$ ). For full scans of western blots from **a** and **c** see Supplemental Figure S6. Data are shown as mean  $\pm$  SD. \* $p < 0.05$ ; \*\* $p < 0.05$

encapsulated siRNA at and above PCX/siRNA (w/w) ratios of 2 (Fig. 5a). Hydrodynamic size and  $\zeta$ -potential of the prepared PCX/siRNA nanoparticles (w/w = 2) were measured by dynamic light scattering. Nanoparticles presented size of  $63.3 \pm 0.9$  nm with low dispersity index (0.14) (Fig. 5b) and positive surface charge with  $\zeta$  potential of  $18.2 \pm 0.7$  mV (Fig. 5c). The morphology of the nanoparticles was analyzed by transmission electron microscopy (TEM). We observed uniform particles with mostly spherical morphology (Fig. 5d). The release of siRNA from the nanoparticles was studied by heparin displacement assay. Nanoparticles completely released siRNA after incubation with heparin concentrations above 120  $\mu$ g/mL (Fig. 5e).

### Runx1 knockdown by PCX/siRunx1 polyplexes

Before testing the ability to deliver siRNA by PCX, we first examined whether PCX can be efficiently internalized by leukemia cells. We incubated *Cbfb-MYH11*<sup>+</sup> leukemia cells with nanoparticles prepared with Alexa Fluor 647-labeled PCX polymers (AF647-PCX) for 72 h. Cells were then treated with a light detergent wash to strip them of cell surface proteins. An antibody against the cell surface receptor KIT, which is highly expressed in *Cbfb-MYH11*<sup>+</sup> leukemia cells, was used as a control for stripping [28]. We found that nearly all PCX-AF647-treated cells (99%) were

fluorescent after stripping and showed no significant difference in the percentage of fluorescent cells compared with unstripped cells. This indicates that the majority of the nanoparticles were efficiently internalized by leukemia cells and that little PCX remained on the extracellular surface. In contrast, in cells stained with the KIT antibody, which is not expected to be internalized, the detergent wash led to the loss of fluorescent signal, indicating that cell surface proteins were effectively stripped from the plasma membrane (Fig. 6a). To evaluate the ability of PCX/siRNA nanoparticles to deliver siRNA to *Cbfb-MYH11*<sup>+</sup> leukemia cells, we formulated PCX with siRNA targeting *Runx1* (PCX/siRunx1) or a negative control siRNA (PCX/siNC). We treated leukemia cells from three independent *Cbfb-MYH11*<sup>+/56M</sup>, *Mxl-Cre*<sup>+</sup> mice with PCX/siRunx1 or PCX/siNC for 6 h and analyzed *Runx1* expression by qRT-PCR. We found that cells treated with PCX/siRunx1 showed a significant decrease in *Runx1* expression (Fig. 6b). To test if the knockdown of *Runx1* using PCX/siRunx1 caused defects on cell survival, we stained the cells treated with PCX/siRunx1 and PCX/siNC with Annexin V. We found that PCX/siRunx1 treatment led to an increase in the percentage of Annexin V<sup>+</sup> cells (average 40.5%,  $\pm 1.6$ ) as compared with the cells treated with PCX/siNC particles (average 36.5%,  $\pm 1.4$ ). In addition, the percentage of Annexin V<sup>+</sup> cells from PCX/siNC treatment was significantly higher than that of

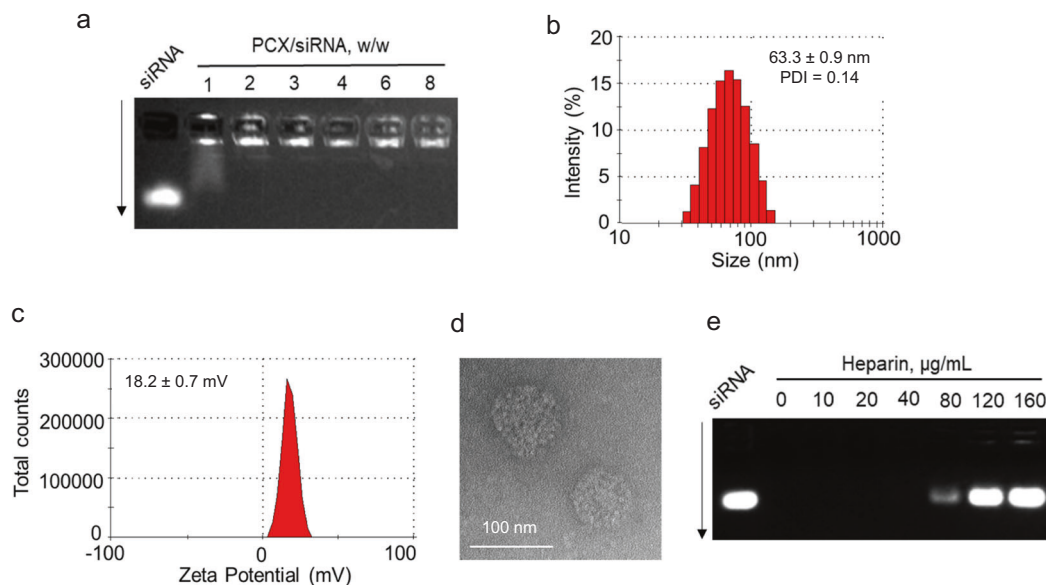


**Fig. 5** Physicochemical characterization of PCX/siRNA nanoparticles. **a** siRNA condensation by PCX using agarose gel electrophoresis. **b** Hydrodynamic size distribution of PCX/siRNA nanoparticles (w/w = 2). **c**  $\zeta$ -potential of PCX/siRNA nanoparticles

(w/w = 2). **d** Transmission electron microscopy (TEM) image of PCX/siRNA nanoparticles (w/w = 2). **e** Heparin induced siRNA release from the PCX/siRNA nanoparticles (w/w = 2) with increasing concentration of heparin

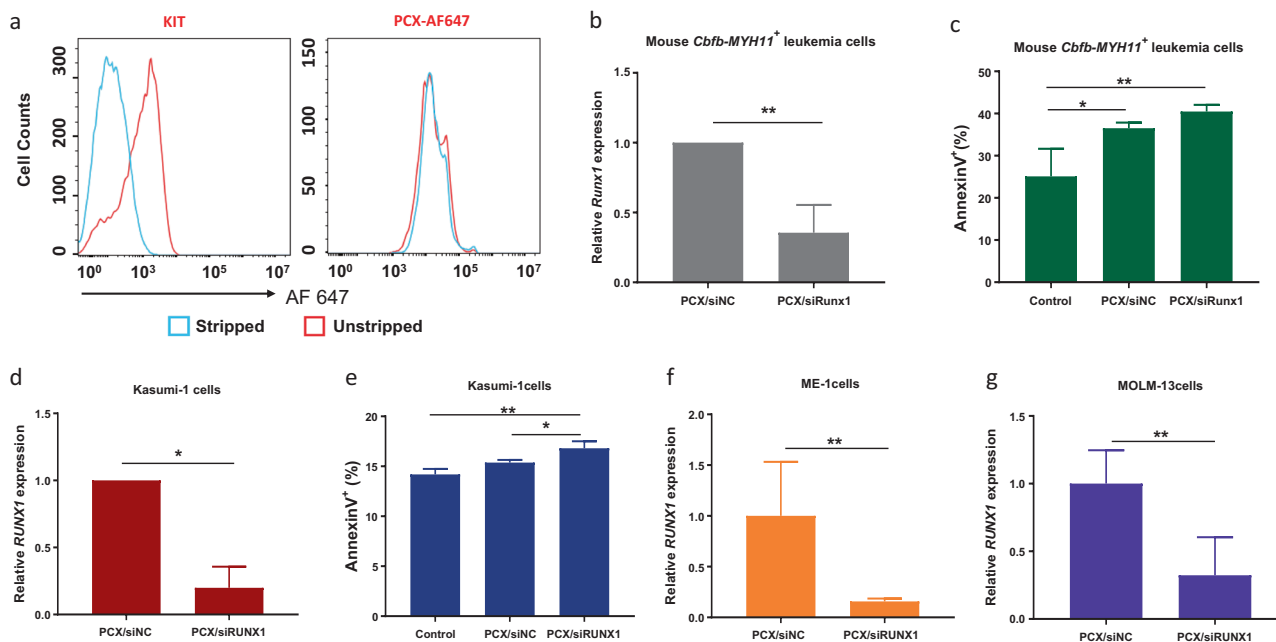


**Fig. 6** Intracellular uptake and gene silencing effects in leukemia cells treated with siRUNX1 delivered by CXCR4-targeted nanoparticles in vitro. **a** FACS plots of the number of cells with Alexa Fluor 647 (AF647) before and after stripping of cells surface proteins and treated with either a labeled antibody against KIT or with AF647-labeled PCX. **b** Bar graph showing the fold change in mRNA expression of *Runx1* in *Cbfb-MYH11*<sup>+</sup> leukemia cells treated with PCX coupled with either Runx1 siRNA (PCX/siRunx1) or non-targeting siRNA (PCX/siNC) for 6 h in culture ( $n = 4$ ). **c** Bar graph showing the percentage of Annexin V<sup>+</sup> leukemia cells either untreated, treated with PCX/siNC,

or treated with PCX/siRunx1 for 24 h in culture ( $n = 3$ ). **d** Bar graph showing the fold change in mRNA expression of *RUNX1* in Kasumi-1 cell line treated with PCX coupled with either RUNX1 siRNA (PCX/siRUNX1) or non-targeting siRNA (PCX/siNC) for 6 h in culture ( $n = 3$ ). **e** Bar graph showing the percentage of Annexin V<sup>+</sup> Kasumi-1 cells either untreated, treated with PCX/siNC, or treated with PCX/siRUNX1 for 6 h in culture ( $n = 3$ ). **f**, **g** Bar graphs showing the fold change in mRNA expression of *RUNX1* in ME-1 and MOLM-13 cells treated with PCX/siNC, or PCX/siRUNX1 for 24 h in culture ( $n = 3$ ). Data are shown as mean  $\pm$  SD. \*  $p < 0.05$ ; \*\*  $p < 0.01$ ; \*\*\*  $p < 0.001$

untreated cells, consistent with our analysis that PCX has anti-leukemia activity on its own (Fig. 6c). Collectively, our results indicate that PCX can efficiently deliver siRNA to *Cbfb-MYH11*<sup>+</sup> leukemia cells in vitro and cause apoptosis.

To test if PCX delivers siRUNX1 to human AML cells, we used Kasumi-1s, ME-1s and the mixed lineage leukemia-rearranged leukemia cell line, MOLM-13, as they have also been shown to require RUNX1 expression for survival [36–38]. We treated cells with PCX/siRUNX1 or PCX/siNC nanoparticles. The expression of RUNX1 was significantly decreased within 6 h in Kasumi-1 cells cultured with PCX/siRUNX1 as compared with those with PCX/siNC (Fig. 6d). In addition, the percentage of Annexin V<sup>+</sup> cells from PCX/siRUNX1 treatment was significantly higher than cells cultured with PCX/siNC in Kasumi-1 cells (Fig. 6e). We also found that the expression of RUNX1 was significantly decreased in both ME-1 and MOLM-13 cells cultured with PCX/siRUNX1 as compared with those with PCX/siNC (Fig. 6f, g), although this decrease in RUNX1 expression was not accompanied by an increase in Annexin V staining in these cells lines (Supplemental Fig. S5). These findings indicate that PCX efficiently delivered siRUNX1 to human leukemia cells. Thus, our study indicates that PCX is able to deliver siRNA targeting important regulators of leukemia cells and has therapeutic potential to treat patients with AML.

## Discussion

Despite the recent development of several targeted inhibitors for the treatment of AML, there remains significant populations of patients with relapsed or refractory disease for whom there are few effective treatment options [39, 40]. This is in part related to the heterogeneity of AML. Unlike many solid tumors, there is not a single driver mutation present in the majority of AML patient samples [8]. siRNA-based therapy has emerged as a novel therapeutic approach for treating AML as it is highly specific and customizable, providing the flexibility of targeting different oncogenes [41–44].

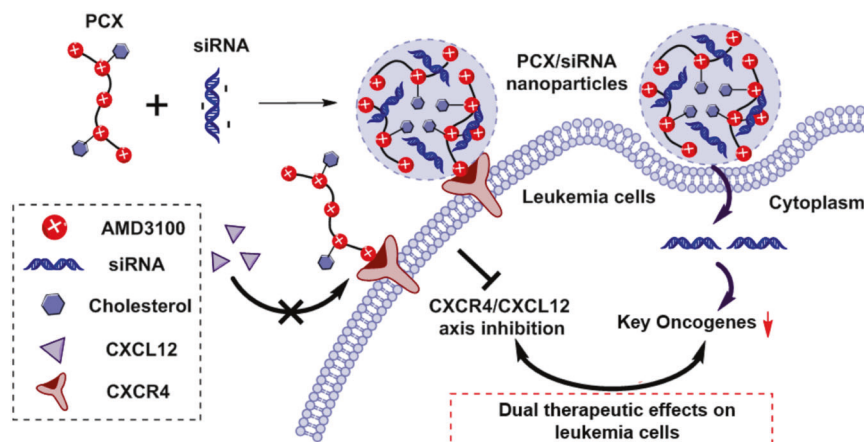
In this study, we characterized a polymeric CXCR4 antagonist (PCX), which is capable of delivering siRNAs in leukemia cells. We showed that PCX has a cytotoxic effect in AML cells in vitro. Our results also suggest that treatment with PCX induces leukemia cell differentiation. Multiple agents have been developed and tested for CXCR4-targeted therapy including the small molecule inhibitor AMD3100 and the peptide CXCR4 inhibitors BKT140 and LY2510924 [34, 45, 46]. Interestingly, when we directly compared PCX with AMD3100, BKT140, and LY2510924, we found that none of the other inhibitors showed anti-leukemic activity in vitro, even at 10–20 times

higher concentrations. This was expected with AMD3100, as previous work has indicated that AMD3100 alone does not affect leukemia cell survival, and that its clinical utility stems from its ability to mobilize leukemia cells out of the protective microenvironment [21]. However, previous studies of using LY2510924 and BKT140 have shown effects on viability and differentiation in AML cells [34, 46]. Although we did not observe such effects in our study, these previous findings imply that the anti-leukemic effects of PCX are likely owing to enhanced inhibition of CXCR4, potentially owing to a multivalency effect. This is further supported by studies using the humanized anti-CXCR4 antibodies Ulocuplumab and PF-0674714, which both exhibit anti-leukemic activity both in vitro and in vivo [47, 48]. However, we cannot rule out the possibility that PCX may have additional CXCR4-independent activities, as well.

Another advantage of PCX is its ability to act as an siRNA delivery vehicle [19, 29]. In this “proof of concept” study, we used RUNX1 as a knockdown target as its expression is required in leukemia cells of multiple different subtypes [36–38, 49, 50]. We found that PCX successfully delivered siRNAs against RUNX1 and caused decreased *RUNX1* expression in both mouse *Cbfb-MYH11*<sup>+</sup> cells and human AML cells. This implies that PCX has potential as a nucleic acid delivery vehicle to AML cells. However, in contrast to previous reports, we did not observe increased cell death with *RUNX1* knockdown in either ME-1s or Molm-13s. Currently, we do not know if this is because *Runx1* was not completely silenced. Although genetic loss or complete knockdown of RUNX1 causes cell death in many AML subtypes, a more recent study showed that moderate level of *RUNX1* expression paradoxically promotes leukemogenesis [28, 36, 51]. Consequently, for use in patients, RUNX1 may not be the most appropriate target for PCX/siRNA nanoparticles. However, as siRNAs are highly customizable, this approach could be used to target other leukemogenic oncogenes. Leukemic fusion genes are a particularly attractive target as they are likely expressed in all leukemia cells in a sample, but not in healthy cells [52].

Based on these data, we propose the following model of action of PCX/siRNA nanoparticles (Fig. 7). PCX inhibits CXCR4, leading to mobilization from bone marrow and increased sensitivity to chemotherapy, similar to AMD3100. However, PCX also causes cell death and differentiation, which further decreases leukemic burden. More importantly, PCX is also able to deliver siRNAs capable of silencing critical oncogenes. Owing to its multifunctionality, PCX has potential for the treatment of patients who cannot tolerate traditional chemotherapy, or whose disease is refractory to such treatments. Collectively, our work indicates that PCX has potential as an effective treatment for patients with AML.

**Fig. 7** Proposed mechanism of action of PCX/siRNA nanoparticles for treatment of acute myeloid leukemia



## Materials and methods

### Synthesis of PCX

Cholesterol-modified polymeric CXCR4 inhibitors PCX (Mw = 16.7 kDa, Mw/Mn = 1.9, cholesterol wt% = 16.8%) were synthesized and characterized as previously described [53]. Succinimidyl ester of Alexa Fluor® 647 carboxylic acid was obtained from Life Technologies (Eugene, OR, USA). Alexa Fluor 647-labeled PCX polymers (AF647-PCX) were prepared according to the manufacturer's instructions and purified by dialysis to remove unreacted free dye. Non-targeting siRNA control (siNC, 5'-UCACAACCUCUA-GAAAGAGUAGA-3'), human RUNX1 siRNA (siRUNX1, 5'-GACAUCGGCAGAAACUAGA UU-3'), and cholesterol-modified mouse Runx1 siRNA (siRunx1, 5'-GCACCUACCAUAGAGCCAUCAACUU-3') were purchased from Dharmacon (Dharmacon, Inc., Chicago, IL, USA). Human RUNX1 siRNA sequence has been described previously [36].

### Mice

This study was performed in accordance with the guidelines established by the Guide for the Care and Use of Laboratory Animals at the National Institutes of Health. All experiments involving mice were approved by the Institutional Animal Care and Use Committee at the University of Nebraska Medical Center. All mice were maintained on a mixed C57Bl6/129SvEv background, were of both sexes, and were at least 6 weeks of age. Mice expressing a conditional allele of full-length *Cbfb-MYH11* (*Cbfb*<sup>+56M</sup>) were paired with the inducible *Mxl-Cre* transgene, and were treated with polyinosinic-polycytidylic acid to induce the expression of *Cbfb-MYH11* as described previously [25]. Mice were sacrificed at the first signs of disease, and leukemia cells from bone marrow or spleen were collected and cryopreserved in 10% dimethylsulfoxide. All experiments

involving mouse cells were performed at least three independent times using samples obtained from at least three independent mice. This sample size was based on previous work showing that samples from three independent mice is sufficient to address potential animal to animal variation. No randomization or exclusion strategies of animal samples were used in this study.

### Cell culture

Kasumi-1 cell line was purchased from the ATCC and maintained in Rosewell Park Memorial Institute (RPMI)-1640 (ATCC, Manassas, VA, USA) supplemented with 20% fetal bovine serum (FBS), 2 mM L-Glutamine and 1% penicillin-streptomycin. ME-1 cell line was kindly provided by Dr. Paul Liu (NHGRI/NIH) and maintained in RPMI-1640 (ATCC) supplemented with 20% FBS, 2 mM L-glutamine, 2.5 of a 10% (w/v) glucose solution, 1% penicillin-streptomycin, 1% sodium pyruvate, and 2.5% 1 M HEPES (4-(2-hydroxyethyl)-1-piperazineethanesulfonic acid). MOLM-13 cell line was purchased from the DSMZ and maintained in RPMI-1640 (ATCC) supplemented with 20% FBS, 2 mM L-Glutamine and 1% penicillin-streptomycin. Mouse leukemia cells were isolated from the spleens of sick animals and were cultured in RPMI-1640 (ATCC), supplemented with 20% FBS ES-Qualified (Life Technologies, Grand Island, NY, USA), 2 mM L-Glutamine, and 1% penicillin-streptomycin. Media for culturing mouse leukemia cells was supplemented with cytokines at the indicated concentration: IL-3 (10 ng/mL; Peprotech, Rocky Hill, NJ, USA), IL-6 (10 ng/mL; Peprotech), and SCF (20 ng/mL; Peprotech), IL-33 (100 ng/mL; Peprotech). HEK293T cells were maintained in Dulbecco's Modified Eagle medium (Corning, Manassas, VA, USA) supplemented with 10% FBS, 2 mM L-Glutamine and 1% penicillin-streptomycin. AMD3100 was from Biochem-partner (Shanghai, China). BKT140 was from GL biotechnology Inc. (Shanghai, China). LY2510924 was

purchased from MCE (MedChem Express, HY-12488, Monmouth Junction, NJ, USA). Colony assays were performed using equal numbers of leukemia cells suspended in Methocult 3434 (StemCell Technologies, Vancouver, BC, Canada) according to the manufacturer's protocol. After 14 days in culture, plates were scored for colony number. All cells were cultured at 37 °C in a humidified 5% CO<sub>2</sub> incubator. No cell line authentication was performed by the authors. Cells were routinely tested for mycoplasma (Mycoalert Plus, Lonza). All experiments involving cell lines were performed at least three independent times.

### Lentiviral production and transduction

HEK293T cells were transfected with third generation lentiviral plasmids which contain DsRed. The viral supernatant was collected 48 h post transfection. For transduction, mouse leukemic spleen cells were incubated with viral supernatant, supplemented with cytokines as described above with the addition of 8 µg/mL polybrene. Cells were spininfected at 2000 rpm for 90 mins, followed by a 6-hour incubation and a second spininfection. Forty-eight hours after the start of transduction, cells were sorted using the DsRed signal.

### Preparation and characterization of nanoparticles

The capability of PCX polymer to condense siRNA was analyzed by electrophoresis in a 2% agarose gel which contained 0.5 µg/mL ethidium bromide. The preparation of PCX/siRNA nanoparticles was performed by adding a predetermined volume of PCX solution to an siRNA solution (20 µM in 10 mM HEPES pH 7.4) to achieve the desired polycation-to-siRNA w/w ratio and vortexing for 10 s. Nanoparticles were further incubated at room temperature for 20 min. Nanoparticles were then loaded (20 µL of the sample containing 0.5 µg of siRNA) into gel wells and run for 20 min at 100 V in 0.5 × Tris/Borate/ethylenediamine-tetraacetic acid buffer. The gels were visualized under ultraviolet illumination with a KODAK Gel Logic 100 imaging system. Hydrodynamic diameter and zeta potential of the nanoparticles were measured by dynamic light scattering using a ZEN3600 Zetasizer Nano-ZS (Malvern Instruments Ltd., Malvern, Worcestershire, UK). The morphology of nanoparticles was observed under TEM (Tecnai G2 Spirit, FEI Company, Houston, TX, USA) using NanoVan® negative staining (Nanoprobes, Yaphank, NY, USA). The release of siRNA from nanoparticles was analyzed by heparin displacement assay. Nanoparticles (w/w = 2) were incubated with increasing concentrations of heparin solution for 30 min at room temperature. The samples were then analyzed by agarose gel electrophoresis.

### Flow cytometry

Mouse leukemia cells isolated from spleen were stained with PE conjugated anti-CSF2RB (559920, BD Pharmingen, Oxford, UK), PE conjugated anti-CXCR4 (561734, BD Pharmingen), allophycocyanin (APC)-conjugated anti-KIT (553356, BD Biosciences, Oxford, UK), BV421 conjugated anti-Mac-1 (562605, BD Biosciences), and BV510 conjugated anti-Gr-1 (563040, BD Biosciences). Cell viability was determined by staining with DAPI. For the measurement of apoptosis, we used the APC-conjugated Annexin V (550475, BD Biosciences). To strip the cells of cell surface proteins, cells were incubated with acid stripping buffer (0.5% acetic acid, 4 M NaCl, pH 3.0) to remove any surface-bound and noninternalized antibody. Cells were analyzed using BD LSRII flow cytometer (BD Biosciences) equipped with FACSDiva software (Becton Dickinson, San Jose, CA, USA). Fluorescence-activated cell sorting data were analyzed by FlowJo software (Tree Star, Ashland, OR, USA).

### RNA isolation and real-time RT-PCR

Total RNA was isolated from cells using Trizol reagent from Invitrogen (Carlsbad, CA, USA) according to the manufacturer's specifications. First strand cDNA synthesis was accomplished using EcoDry Premix (Clontech, Mountain View, CA). qRT-PCR was performed using Maxima SYBR Green/ROX qPCR Master Mix (Thermo Fisher Scientific). The real-time PCR was run in a StepOnePlus Real-Time PCR System (Invitrogen). The oligonucleotide primers used for PCR are shown in Supplemental Table S1 [36, 54].

### Western blotting

Mouse leukemia cells were lysed with RIPA buffer (50 mM Tris-HCl pH 8.0, 150 mM NaCl, 1% Triton, 0.5% deoxycholate, and 0.1% sodium dodecyl sulphate), supplemented with a protease inhibitor (Roche, Penzberg, Germany). Samples were run on 4–12% Bis-Tris gel (Invitrogen), transferred to polyvinylidene difluoride membrane (NOVEX, San Diego, CA, USA). The membrane was incubated with the primary antibody overnight, followed by 1-hour incubation with horseradish peroxidase-conjugated anti-rabbit or anti-mouse secondary antibodies at room temperature, washed and incubated with chemiluminescence reagent (Thermo Fisher Scientific) and then exposed to film. The following primary antibodies were used for western blotting: RUNX1 (39000, Active Motif, Carlsbad, CA, USA) and GAPDH (AM4300, Ambion, Austin, TX, USA).

## Histological staining

Cells were affixed to Surgipath Apex Superior Adhesive Slides (Leica Microsystems, Weztlar, Germany) using a Shandon Cytospin III cytocentrifuge for 5 min at 1000 rpm. Slides were stained using Protocol Hema 3 Wright–Giemsa stain (Thermo Fisher Scientific) according to the manufacturer's protocol and were examined in a blinded manner using an Olympus BX51 microscope at  $\times 100$  magnification.

## Statistical analysis

All statistical analysis was conducted using the Graph Pad 7.0 Prism software (GraphPad Software, La Jolla, CA, USA). Data are represented as mean values  $\pm$  standard deviation. The significance of difference between two groups was determined by Student's *t* test or the Mann–Whitney *U*-test. *F* testing was performed to confirm equal variance. More than two groups were compared using a one-way analysis of variance or Kruskal–Wallis test, and Brown–Forsythe test was used to check equal variance.  $p < 0.05$  was considered to be statistically significant.

**Acknowledgements** We thank UNMC Flow Cytometry Research and the UNMC Center for Comparative Medicine. This work was supported by the state of Nebraska through LB606 and the Nebraska Pediatric Cancer Research Group.

**Author contributions** Y.W., Y.X., D.O., and R.K.H. conceived of and designed the study; Y.W., Y.X., J.W., Y.H., L.R., and M.B. performed experiments; C.A. performed histological evaluations. Y.W., Y.X., D. O., and R.K.H. wrote the manuscript.

## Compliance with ethical standards

**Conflict of interest** The authors declare no competing financial interest.

**Publisher's note:** Springer Nature remains neutral with regard to jurisdictional claims in published maps and institutional affiliations.

## References

- Briot T, Roger E, Thepot S, Lagarce F. Advances in treatment formulations for acute myeloid leukemia. *Drug Discov Today*. 2018;23:1936–49.
- Dohner H, Weisdorf DJ, Bloomfield CD. Acute myeloid leukemia. *N Engl J Med*. 2015;373:1136–52.
- Papaemmanuil E, Gerstung M, Bullinger L, Gaidzik VI, Paschka P, Roberts ND, et al. Genomic classification and prognosis in acute myeloid leukemia. *N Engl J Med*. 2016;374:2209–21.
- Saultz JN, Garzon R. Acute myeloid leukemia: a concise review. *J Clin Med*. 2016;5:E33.
- De Kouchkovsky I, Abdul-Hay M. 'Acute myeloid leukemia: a comprehensive review and 2016 update'. *Blood Cancer J*. 2016;6:e441.
- Andresen V, Gjertsen BT. Drug repurposing for the treatment of acute myeloid leukemia. *Front Med (Lausanne)*. 2017;4:211.
- Alexandrov LB, Nik-Zainal S, Wedge DC, Aparicio SA, Behjati S, Biankin AV, et al. Signatures of mutational processes in human cancer. *Nature*. 2013;500:415–21.
- Cancer Genome Atlas Research N, Ley TJ, Miller C, Ding L, Raphael BJ, Mungall AJ, et al. Genomic and epigenomic landscapes of adult de novo acute myeloid leukemia. *N Engl J Med*. 2013;368:2059–74.
- Cunningham L, Finckbeiner S, Hyde RK, Southall N, Marugan J, Yedavalli VR, et al. Identification of benzodiazepine Ro5-3335 as an inhibitor of CBF leukemia through quantitative high throughput screen against RUNX1-CBFBeta interaction. *Proc Natl Acad Sci USA*. 2012;109:14592–7.
- Illendula A, Pulikkan JA, Zong H, Grembecka J, Xue L, Sen S, et al. Chemical biology. A small-molecule inhibitor of the aberrant transcription factor CBFBeta-SMMHC delays leukemia in mice. *Science*. 2015;347:779–84.
- Illendula A, Gilmour J, Grembecka J, Tirumala VSS, Boulton A, Kuntimaddi A, et al. Small molecule inhibitor of CBFBeta-RUNX binding for RUNX transcription factor driven cancers. *EBioMedicine*. 2016;8:117–31.
- Seton-Rogers S. Therapeutics: siRNAs jump the hurdle. *Nat Rev Cancer*. 2012;12:376–7.
- Wilda M, Fuchs U, Wossmann W, Borkhardt A. Killing of leukemic cells with a BCR/ABL fusion gene by RNA interference (RNAi). *Oncogene*. 2002;21:5716–24.
- Kaur K, Rath G, Chandra S, Singh R, Goyal AK. Chemotherapy with si-RNA and anti-cancer drugs. *Curr Drug Deliv*. 2018;15:300–11.
- Devi GR. siRNA-based approaches in cancer therapy. *Cancer Gene Ther*. 2006;13:819–29.
- Deng Y, Wang CC, Choy KW, Du Q, Chen J, Wang Q, et al. Therapeutic potentials of gene silencing by RNA interference: principles, challenges, and new strategies. *Gene*. 2014;538:217–27.
- Xin Y, Huang M, Guo WW, Huang Q, Zhang LZ, Jiang G. Nano-based delivery of RNAi in cancer therapy. *Mol Cancer*. 2017;16:134.
- Li J, Zhu Y, Hazeldine ST, Li C, Oupicky D. Dual-function CXCR4 antagonist polyplexes to deliver gene therapy and inhibit cancer cell invasion. *Angew Chem Int Ed Engl*. 2012;51:8740–3.
- Wang Y, Li J, Chen Y, Oupicky D. Balancing polymer hydrophobicity for ligand presentation and siRNA delivery in dual function CXCR4 inhibiting polyplexes. *Biomater Sci*. 2015;3:1114–23.
- Xie Y, Wang Y, Li J, Hang Y, Oupicky D. Promise of chemokine network-targeted nanoparticles in combination nucleic acid therapies of metastatic cancer. *Wiley Interdiscip Rev Nanomed Nanobiotechnol*. 2018;11:e1528.
- Nervi B, Ramirez P, Rettig MP, Uy GL, Holt MS, Ritchey JK, et al. Chemosensitization of acute myeloid leukemia (AML) following mobilization by the CXCR4 antagonist AMD3100. *Blood*. 2009;113:6206–14.
- Uy GL, Rettig MP, Motabi IH, McFarland K, Trinkaus KM, Hladnik LM, et al. A phase 1/2 study of chemosensitization with the CXCR4 antagonist plerixafor in relapsed or refractory acute myeloid leukemia. *Blood*. 2012;119:3917–24.
- Cooper TM, Sison EAR, Baker SD, Li L, Ahmed A, Trippett T, et al. A phase 1 study of the CXCR4 antagonist plerixafor in combination with high-dose cytarabine and etoposide in children with relapsed or refractory acute leukemias or myelodysplastic syndrome: a pediatric oncology experimental therapeutics investigators' Consortium study (POE 10-03). *Pediatr Blood Cancer*. 2017;64. <https://doi.org/10.1002/pbc.26414>.

24. Martinez-Cuadron D, Boluda B, Martinez P, Bergua J, Rodriguez-Veiga R, Esteve J, et al. A phase I-II study of plerixafor in combination with fludarabine, idarubicin, cytarabine, and G-CSF (PLERIFLAG regimen) for the treatment of patients with the first early-relapsed or refractory acute myeloid leukemia. *Ann Hematol.* 2018;97:763–72.
25. Kuo YH, Landrette SF, Heilman SA, Perrat PN, Garrett L, Liu PP, et al. Cbf beta-SMMHC induces distinct abnormal myeloid progenitors able to develop acute myeloid leukemia. *Cancer Cell.* 2006;9:57–68.
26. Hyde RK, Zhao L, Alemu L, Liu PP. Runx1 is required for hematopoietic defects and leukemogenesis in Cbfb-MYH11 knock-in mice. *Leukemia.* 2015;29:1771–8.
27. Wang Y, Richter L, Becker M, Amador C, Hyde RK. IL1RL1 is dynamically expressed on Cbfb-MYH11(+) leukemia stem cells and promotes cell survival. *Sci Rep.* 2019;9:1729.
28. Hyde RK, Kamikubo Y, Anderson S, Kirby M, Alemu L, Zhao L, et al. Cbfb/Runx1 repression-independent blockage of differentiation and accumulation of Csf2rb-expressing cells by Cbfb-MYH11. *Blood.* 2010;115:1433–43.
29. Xie Y, Wang Y, Li J, Hang Y, Jaramillo L, Wehrkamp CJ, et al. Cholangiocarcinoma therapy with nanoparticles that combine downregulation of MicroRNA-210 with inhibition of cancer cell invasiveness. *Theranostics.* 2018;8:4305–20.
30. Juarez J, Bradstock KF, Gottlieb DJ, Bendall LJ. Effects of inhibitors of the chemokine receptor CXCR4 on acute lymphoblastic leukemia cells in vitro. *Leukemia.* 2003;17:1294–300.
31. Beider K, Begin M, Abraham M, Wald H, Weiss ID, Wald O, et al. CXCR4 antagonist 4F-benzoyl-TN14003 inhibits leukemia and multiple myeloma tumor growth. *Exp Hematol.* 2011;39:282–92.
32. Zhang Y, Patel S, Abdelouahab H, Wittner M, Willekens C, Shen S, et al. CXCR4 inhibitors selectively eliminate CXCR4-expressing human acute myeloid leukemia cells in NOG mouse model. *Cell Death Dis.* 2012;3:e396.
33. Galsky MD, Vogelzang NJ, Conkling P, Raddad E, Polzer J, Roberson S, et al. A phase I trial of LY2510924, a CXCR4 peptide antagonist, in patients with advanced cancer. *Clin Cancer Res.* 2014;20:3581–8.
34. Cho BS, Zeng Z, Mu H, Wang Z, Konoplev S, McQueen T, et al. Antileukemia activity of the novel peptidic CXCR4 antagonist LY2510924 as monotherapy and in combination with chemotherapy. *Blood.* 2015;126:222–32.
35. Peng SB, Zhang X, Paul D, Kays LM, Gough W, Stewart J, et al. Identification of LY2510924, a novel cyclic peptide CXCR4 antagonist that exhibits antitumor activities in solid tumor and breast cancer metastatic models. *Mol Cancer Ther.* 2015;14:480–90.
36. Ben-Ami O, Friedman D, Leshkowitz D, Goldenberg D, Orlovsky K, Pencovich N, et al. Addiction of t(8;21) and inv(16) acute myeloid leukemia to native RUNX1. *Cell Rep.* 2013;4:1131–43.
37. Wilkinson AC, Ballabio E, Geng H, North P, Tapia M, Kerry J, et al. RUNX1 is a key target in t(4;11) leukemias that contributes to gene activation through an AF4-MLL complex interaction. *Cell Rep.* 2013;3:116–27.
38. Morita K, Suzuki K, Maeda S, Matsuo A, Mitsuda Y, Tokushige C, et al. Genetic regulation of the RUNX transcription factor family has antitumor effects. *J Clin Invest.* 2017;127:2815–28.
39. Gu R, Yang X, Wei H. Molecular landscape and targeted therapy of acute myeloid leukemia. *Biomark Res.* 2018;6:32.
40. Luppi M, Fabbiano F, Visani G, Martinelli G, Venditti A. Novel agents for acute myeloid leukemia. *Cancers (Basel).* 2018;10:E429.
41. Cioca DP, Aoki Y, Kiyosawa K. RNA interference is a functional pathway with therapeutic potential in human myeloid leukemia cell lines. *Cancer Gene Ther.* 2003;10:125–33.
42. Landry B, Aliabadi HM, Samuel A, Gul-Uludag H, Jiang X, Kutsch O, et al. Effective non-viral delivery of siRNA to acute myeloid leukemia cells with lipid-substituted polyethylenimines. *PLoS ONE.* 2012;7:e44197.
43. Gul-Uludag H, Valencia-Serna J, Kucharski C, Marquez-Curtis LA, Jiang X, Larratt L, et al. Polymeric nanoparticle-mediated silencing of CD44 receptor in CD34+ acute myeloid leukemia cells. *Leuk Res.* 2014;38:1299–308.
44. Uludag H, Landry B, Valencia-Serna J, Remant-Bahadur KC, Meneksedag-Erol D. Current attempts to implement siRNA-based RNAi in leukemia models. *Drug Discov Today.* 2016;21:1412–20.
45. Azab AK, Runnels JM, Pitsillides C, Moreau AS, Azab F, Leleu X, et al. CXCR4 inhibitor AMD3100 disrupts the interaction of multiple myeloma cells with the bone marrow microenvironment and enhances their sensitivity to therapy. *Blood.* 2009;113:4341–51.
46. Abraham M, Klein S, Bulvik B, Wald H, Weiss ID, Olam D, et al. The CXCR4 inhibitor BL-8040 induces the apoptosis of AML blasts by downregulating ERK, BCL-2, MCL-1 and cyclin-D1 via altered miR-15a/16-1 expression. *Leukemia.* 2017;31:2336–46.
47. Kuhne MR, Mulvey T, Belanger B, Chen S, Pan C, Chong C, et al. BMS-936564/MDX-1338: a fully human anti-CXCR4 antibody induces apoptosis in vitro and shows antitumor activity in vivo in hematologic malignancies. *Clin Cancer Res.* 2013;19:357–66.
48. Liu SH, Gu Y, Pascual B, Yan Z, Hallin M, Zhang C, et al. A novel CXCR4 antagonist IgG1 antibody (PF-06747143) for the treatment of hematologic malignancies. *Blood Adv.* 2017;1:1088–100.
49. Hyde RK, Liu P, Friedman AD. RUNX1 and CBFbeta mutations and activities of their wild-type alleles in AML. *Adv Exp Med Biol.* 2017;962:265–82.
50. Goyama S, Schibler J, Cunningham L, Zhang Y, Rao Y, Nishimoto N, et al. Transcription factor RUNX1 promotes survival of acute myeloid leukemia cells. *J Clin Invest.* 2013;123:3876–88.
51. Morita K, Maeda S, Suzuki K, Kiyose H, Taniguchi J, Liu PP, et al. Paradoxical enhancement of leukemogenesis in acute myeloid leukemia with moderately attenuated RUNX1 expressions. *Blood Adv.* 2017;1:1440–51.
52. Wang Y, Wu N, Liu D, Jin Y. Recurrent fusion genes in leukemia: an attractive target for diagnosis and treatment. *Curr Genom.* 2017;18:378–84.
53. Wang Y, Kumar S, Rachagani S, Sajja BR, Xie Y, Hang Y, et al. Polyplex-mediated inhibition of chemokine receptor CXCR4 and chromatin-remodeling enzyme NCOA3 impedes pancreatic cancer progression and metastasis. *Biomaterials.* 2016;101:108–20.
54. Kuo YH, Zaidi SK, Gornostaeva S, Komori T, Stein GS, Castilla LH. Runx2 induces acute myeloid leukemia in cooperation with Cbfbeta-SMMHC in mice. *Blood.* 2009;113:3323–32.